



RESEARCH PAPERS

Poly(vinyl alcohol)/ulvan electrospun nanofibers thermally-crosslinked to produce a water stable biomaterial

Luisa Elena Mejía Agüero^{a,b}, Adriana Freire Lubambo^c, Cyro Ketzer Saul^c,
Beatriz Franco Silva^b, Rilton Alves de Freitas^d, Franciely Grose Colodi^b,
Maria Eugênia Rabello Duarte^b, Miguel Daniel Nosedá^{b*}

^aPostgraduate Program in Bioprocesses Engineering and Biotechnology, Federal University of Paraná - UFPR, Curitiba, PR, Brazil

^bDepartment of Biochemistry and Molecular Biology, Universidade Federal do Paraná - UFPR, Curitiba, PR, Brazil

^cLITS, Physics Department, Universidade Federal do Paraná - UFPR, P.O. Box 19044, Centro Politecnico, Curitiba, PR, Brazil

^dBioPol, Pharmacy Department, Universidade Federal do Paraná - UFPR, Curitiba, PR, Brazil

Highlights

- A nanofibrous biomaterial was produced by electrospinning a PVA/ulvan aqueous system
- The ulvan-based nanofiber mat was characterized by FTIR and scanning electron microscopy
- The PVA/ulvan electrospun mat was submitted to thermal treatment (180 °C/60 min)
- The thermally-crosslinked nanofiber mat was stable in water for at least 3 hours
- The thermally-crosslinked PVA/ulvan nanofiber mat showed metal ion binding capacity

Received 05 July, 2023; Accepted 03 November, 2023.

KEYWORDS

Electrospinning;
Nanofibers;
Seaweed;
Sulfated
polysaccharide;
Thermal crosslinking;
Ulva fasciata.

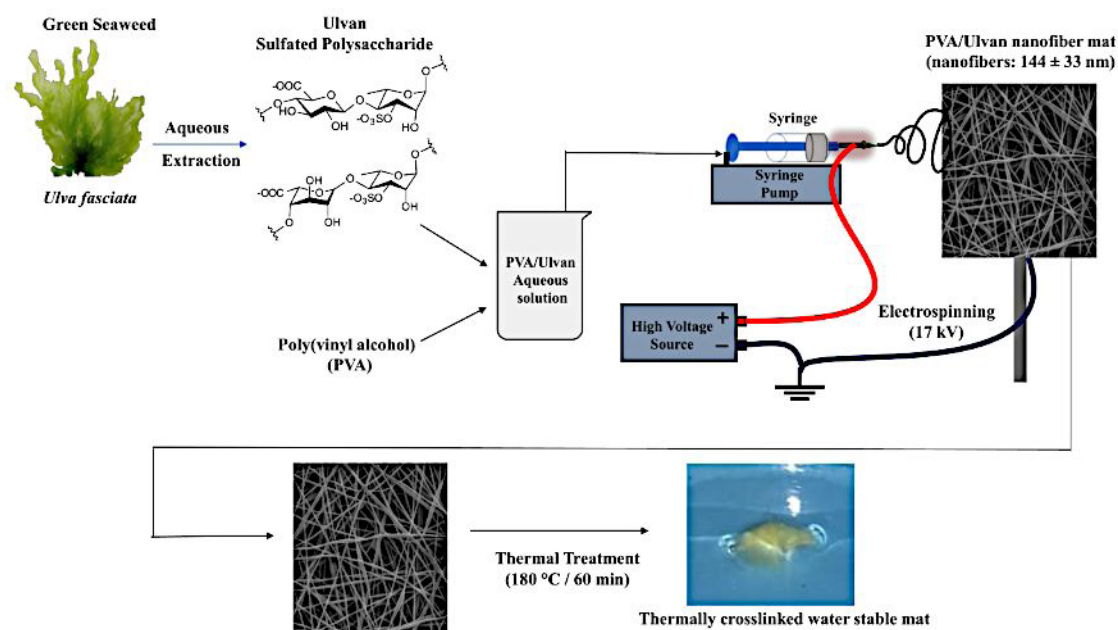
Abstract: Ulvan is the main sulfated polysaccharide isolated from green seaweeds of the genus *Ulva*, showing several biological properties. A fibrous ulvan-based mat exhibiting nanofibers with an average diameter of 144 ± 33 nm, was fabricated from electrospun of an aqueous mixture, composed by poly(vinyl alcohol) (PVA) and ulvan in a 5:2 mass ratio (PVA5U2). As expected from its composition, the PVA5U2 mat readily disintegrated upon contact with water, limiting potential uses. For this reason, mat stabilization against water exposition as well as keeping ulvan functional groups availability in the biomaterial, as fundamental aspects for functionalization purposes, became the main objectives of this work. To achieve them, thermal crosslinking (180 °C/60 min), instead of chemical crosslinking, was used for the first time in this type of biomaterial, modulating the poor stability of the ulvan-based electrospun mat in water and preventing the formation of polysaccharides crosslinking complexes during the stabilization treatment. Infrared spectroscopy and scanning electron microscopy were used to characterize the PVA5U2 mat and the thermally-crosslinked PVA5U2 mat, evidencing the presence of nanofibers and ulvan functional groups. Nanofibers increased 30% in diameter after 180 min of water exposition. The PVA5U2 mat exhibit characteristics that turn them into a versatile biotechnological biomaterial.

*Corresponding author.

E-mail: mdn@ufpr.br (M. D. Nosedá)



Graphical Abstract



Introduction

In the field of biotechnology, the replacement of synthetic materials with natural polymers has received great attention, considering the advantages associated with this change: biocompatibility, biodegradability, low antigen response (vegetal sources), renewable character and low cost (Morelli & Chiellini, 2010; Jesus Raposo et al., 2015; Cunha & Grenha, 2016; Alves et al., 2013).

Within the universe of polysaccharides that draw attention to replace synthetic materials, those obtained from seaweeds have emerged as interesting options, once they present the above mentioned characteristics and have been described as bioactive compounds, with outstanding potential use in different fields: biomedical, food science technology, environmental, cosmetic, and pharmacological (Sari-Chmaysem et al., 2019; Jesus Raposo et al., 2015; Carvalho et al., 2018; Colodi et al., 2021; Cassolato et al., 2008). Some of these polysaccharides, such as carrageenan, alginate, and ulvan, have also been used for the production of nanofibers, one of the major goals in nanotechnology (Vigani et al., 2018; Toskas et al., 2011; Terezaki et al., 2022; Shen & Hsieh, 2014; Mirtič et al., 2019; Madany et al., 2021; Kikionis et al., 2015; Daemi et al., 2018; Amjadi et al., 2020).

The interest in nanofibers relies on its high surface area to volume ratio which allows different biotechnological applications (Xue et al., 2019; Wani et al., 2017; Vass et al., 2020; Ramakrishna et al., 2006; Phan et al., 2021; Persano et al., 2013; Greiner & Wendorff, 2007; Gibson et al., 2001; Bhardwaj & Kundu, 2010). Nanofibers can be produced by different methods, among which the electrospinning technique has been highlighted due to its low cost, simple fashion and relatively high production rate (Schiffman & Schauer, 2008; Ramakrishna et al., 2006; Barnes et al.,

2007). This technique has been used for the development of algal polysaccharide-based nanofibers showing interesting characteristics from a biotechnological point of view (Vigani et al., 2018; Toskas et al., 2011; Terezaki et al., 2022; Shen & Hsieh, 2014; Madany et al., 2021; Kikionis et al., 2022; Daemi et al., 2018). As a prominent representative of polysaccharides obtained from seaweeds, ulvan appears as a water soluble sulfated polysaccharide that exhibits a unique chemical structure characterized by numerous charged groups, which has been associated with interesting properties, such as: anticoagulant, antithrombotic, cancer preventive, anti-inflammatory, antihyperlipidemic, antioxidant, and heavy metals chelation (Webster et al., 1997; Tziveleka et al., 2019; Terezaki et al., 2022; Jesus Raposo et al., 2015; Carvalho et al., 2018; Cunha & Grenha, 2016).

The production of spun fibers from pure marine polysaccharide (i.e. ulvan) represents a real challenge that has been deeply discussed in the review of Mejía Agüero et al. (2022). Consequently, the production of ulvan-based nanofibers using the electrospinning technique, emerges as an alternative that has been barely explored in the literature (Toskas et al., 2011; Terezaki et al., 2022; Madany et al., 2021; Kikionis et al., 2015, 2022; Hwang et al., 2023). To face the drawback associated with the low stability in aqueous media, some methods of crosslinking have been used to prevent dispersion of these materials in aqueous medium (Shen & Hsieh, 2014; Panzavolta et al., 2011; Morelli & Chiellini, 2010; Daemi et al., 2018; Alves et al., 2012). Among them, chemical crosslinking has been highly used for its versatility and good mechanical stability, but in some cases, with a handicap of using toxic compounds (Patil, 2008) and exhibiting irreversible character due to covalent bonds formed, which in some cases, have been referred as permanent barriers for further functionalization (Saravanakumar et al., 2012).

During a chemical crosslinking, some polysaccharide functional groups may be compromised, thus limiting its versatility of use to different degrees. It is worth to mention that hydroxyl, carboxyl and sulfate have been mentioned as important groups during the functionalizing process (Schiffman & Schauer, 2008; Ma et al., 2015; Carvalho et al., 2018; Cunha & Grenha, 2016) of different polysaccharide-based materials, for applications as filters to remove cationic dyes and heavy metal ions (Ma et al., 2015; Li et al., 2020) carriers for selective drug delivery (Saravanakumar et al., 2012; Alves et al., 2012), and wound dressing (Tziveleka et al., 2018; Terezaki et al., 2022; Kikionis et al., 2022).

Based on the previous background, this work proposes the production of an electrospun ulvan-based material, preserving the original polysaccharide functional groups in the final material. It is envisaged that the mat produced in this study may find application through its chelating capacity. For these reasons, the present work deals with the production of a novel electrospun ulvan-based biomaterial, employing a physical process to make it stable in aqueous media, avoiding its instantaneous solubilization and ensuring dilution rates that allow functional uses with the advantage of not using toxic compounds as it could happen in chemical crosslinks.

Materials and methods

Seaweed

Samples of *Ulva fasciata* Delile (Ulvales, Chlorophyta) were collected in Florianópolis (27° 35' 49" S and 48° 32' 58" W) Santa Catarina State, Brazil in May 2013, and identified by Professor Franciane Maria Pellizari UNESPAR, Paranaguá (Paraná State, Brazil). The study performed with this biological material was regulated and authorized by Sistema Nacional de Gestão do Patrimônio Genético e do Conhecimento Tradicional Associado (SisGen), under protocol A41FD6D.

Poly(vinyl alcohol) (PVA)

PVA employed in this research was in the powder form supplied by Dinâmica (batch no. 94332, Londrina, Brazil), and used without further purification. The supplier informed a mass average molar mass (M_w) of 72,000 g.mol⁻¹ and 87-89% of hydrolysis.

Other materials

Ultra-purified water was produced employing an Ultra Purifier Equipment (Gehaka, Master All), equipped with: inlet filter; activated carbon filter (10"); deionizing filter; microbiological filter; reverse osmosis membrane and the UV light Lamp. Ultrapure water was used as the solvent aqueous system. Deuterated water (D₂O) (Cambridge Isotope Laboratories, Inc.), dimethyl-d₆ sulfoxide (Me₂SO-d₆) (Sigma Aldrich) and acetone (Sigma Aldrich) were used for Nuclear Magnetic Resonance (NMR) analyses. All chemicals and reagents used were of analytical grade.

Polysaccharide extraction

Seaweed samples were processed to perform polysaccharide extraction. The ulvan (U) was obtained as described by de Carvalho et al. (2018) and employed as the working fraction. Details about protocols of extraction and purification can be found in Supplementary Material.

Polysaccharide chemical characterization

The U mass average molar mass (M_w) was determined by High-Performance Size Exclusion Chromatograph (HPSEC). The monosaccharide composition of U (Taylor & Conrad, 1972; Cassolato et al., 2008; Carpita & Shea, 1990; Anderson & Stone, 1985) was performed by Gas Chromatography-Mass Spectrometry (GC-MS). The contents of protein, carbohydrate, sulfate and uronic acids of U were determined according to Lowry et al. (1951); Filisetti-Cozzi & Carpita (1991); Dubois et al. (1956); Dodgson & Price (1962), respectively. Further details about protocols of characterization are described in Colodi et al. (2021).

PVA: U blends for electrospinning

PVA and U solutions were prepared separately. The PVA solutions were prepared in glass bottles and stirred at 80-90 °C until total dissolution. Sequentially, the PVA solutions were mixed (50:50) with U solutions to produce PVA: U blends of several mass ratios. The working PVA:U mass ratio (5:2) was selected based on the spinnable character of the blend and uniformity of the fibers.

Spectroscopic methods

Nuclear Magnetic Resonance (NMR)

¹H NMR analyses of U (2% wt), PVA (5% wt), and PVA5U2 solutions were performed at 70 °C, on a Bruker Advance DRX400 NMR spectrometer equipped with a 5-mm multinuclear inverse detection probe, and a base frequency of 400 MHz for ¹H nucleus. All samples were dissolved in 99% deuterated water, using acetone as the internal reference (¹H: 2.23 ppm). ¹H NMR analysis was also performed for the PVA dissolved in Me₂SO-d₆. The NMR spectra were analyzed using Topspin 4.0.6.

Attenuated Total Reflectance - Fourier Transform Infrared analyses (ATR-FTIR)

ATR-FTIR analyses were performed using a Fourier Transform Infrared ALPHA Spectrometer (Bruker, Germany) with 4-25 μm Mid IR, 4000-400 cm⁻¹, 24 scans and 4 cm⁻¹ of spectral resolution. To obtain the FTIR spectra, the dialyzed U extract, PVA commercial powder, and the PVA5U2 nanofiber mat were placed in contact with the laser using a Platinum ATR module.

Rheological and surface tension measurements

Rheological measurements of U, PVA, and PVA5U2 solutions were carried out using a Rheometer HAAKE RheoStress

(Thermo Fisher, Germany), equipped with a water bath temperature controller, and using a cone and plate probe (cone diameter 60 mm, angle 2° and gap of 0.105 mm). The viscoelastic properties of PVA: U systems, given by the elastic (G') and viscous modulus (G''), were measured over a frequency range of 0.01-100 Hz, at linear viscoelastic region. Viscosity and thixotropy (hysteresis in up-down flow curves) were determined using a shear rate over a range from 0.1 to 100 s^{-1} during 300 s, remaining 30 s at 100 s^{-1} , and from 100 to 0.1 s^{-1} . The graphs were constructed considering the equipment sensitivity, given by the minimum torque of 5 $\mu N m$. The border effect on the sample rheological behavior was also determined modifying the geometry gap, and further details can be found in the Supplementary Material. All rheological analyses were performed at 20.0 °C \pm 0.2 °C.

Surface tension was determined using a surface tensiometer (Dataphysics Instruments GmbH contact Angle System OCA 15, Germany), employing a Hamilton syringe (500 μL) with a needle of 0.91 mm of external diameter and 38.1 mm of length. The sample density was determined and registered in the program, before each surface tension measurement at 20 °C. Ultrapure water was employed to calibrate the equipment at 72.8 $mN m^{-1}$. Measurements were performed at rate 1.00 $\mu L \cdot seg^{-1}$ after 10 s of the drop formation. The results were calculated from the average of five values for each test.

Electrospinning conditions

Stubs coated with copper double side adhesive tape were attached on the top of an aluminum collector disk to collect the electrospun composite nanofibers. A 2.5 mL Hamilton syringe was loaded with the polymeric solution, placed into a syringe pump, and the flow rate set to 2.5 + 0.2 $\mu L \cdot min^{-1}$. The voltage source was connected to the blunt syringe needle (+) and the aluminum collector disk (−), and adjusted to 17 + 1 kV until a stable Taylor cone was obtained. The distance between the syringe tip and the collector was of 12 cm, the room temperature of 20 °C \pm 2 and relative humidity of 39% \pm 1.

Scanning Electron Microscopy (SEM) analysis

The spun nanofibers were dried at room temperature, maintained in desiccator under reduced pressure and covered with gold plating in a Balzers SCD030 equipment. A VEGA3 LMU (TESCAN, Czech Republic) and a JSM 6360-LV (JEOL, Japan) Scanning Electron Microscopes (SEM), were used to analyze the morphology and to determine the mean diameter of PVA5U2 electrospun nanofibers. The fibers were examined at an accelerating voltage of 15.0 kV and magnifications from 500X to 20,000 X. The mean fiber diameter was obtained by measurement of 50 fibers (distributed in four quadrants along the micrograph).

Stabilization of fibers in water

As a first approach to stabilize fibers in water, the PVA5U2 electrospun mat was subjected to thermal crosslinking employing dry heat in a drying oven (160 °C for 30 min), following the method of Pelipenko et al. (2013).

Afterward, some modifications to the original method of Pelipenko et al. (2013) were introduced, by using different time-temperature combination treatments. Rynkowska et al. (2019) pointed out the temperature as a factor influencing the crosslinking efficiency. Taking it into consideration, crosslinking temperature increases were performed in this work (170 or 180 °C for 30 min), to evaluate the effect of higher temperatures on the water stability of PVA5U2 mat. Subsequently, an increase in the time of treatment was also considered (60 min) (Riyajan et al., 2009).

The proper crosslinking treatment was selected considering the results obtained by direct observation (tendency to acquire jelly foil aspect during the water immersion) and SEM analysis of the crosslinked mat before and after immersed in distilled water for different time periods (10, 30, 60, 120, and 180 min).

At the end of each immersion time, the mat water excess was removed with filter paper and maintained in desiccator under reduced pressure, at room temperature. Prior to SEM analysis, samples were fixed with glutaraldehyde and dehydrated in increasing concentrations of ethyl alcohol (50, 60, 70, 80, 90, and 100%). The mat was maintained for 15 min in each of the ethyl alcohol solutions. Afterward, the samples were treated as described in the Scanning Electron Microscopy (SEM) analyses section, to determine the characteristics and stability of nanofibers.

PVA5U2 mat swelling and dissolution degree measurements

The PVA5U2 spun mat was dried under vacuum and weighted repeatedly until constant weight, obtaining a dried mat (m_{dry}). Subsequently, the PVA5U2 mat swelling was performed in water, at room temperature. The mat water excess was removed with filter paper and the water uptake was calculated from the mass gain between the m_{dry} and the mat equilibrated in water (m_{wet}). The PVA5U2 mat mass swelling degree (SD) in water was calculated according to the following equation (Rynkowska et al., 2019):

$$SD(g \text{ solvent} / g \text{ dry mat}) = (m_{wet} - m_{dry} / m_{dry}) \quad (1)$$

The dissolution degree was evaluated in terms of the mat weight loss, and calculated as the difference between m_{dry} and the mat taken from the water. The mat water excess was removed with filter paper and dried under vacuum (up to constant weight). The SD and dissolution degree of the PVA5U2 were determined considering the following immersion times: 10, 30, 60, 120 and 180 min.

Metal adsorption

A volume of 50 μL of 2 mol/L $FeCl_3 \cdot H_2O$ solution was added to small glass bottles containing PVA5U2 crosslinked mats (0.0058 g). The small glass bottles were placed in a water bath and stirred at 50 °C for 40 min. Then, the mat was taken from the solution and maintained in the desiccator under reduced pressure. SEM and ATR-FTIR analyses were performed to evaluate the presence of fibers, as well as, changes in the

PVA5U2 crosslinked mat spectrum. The method was adapted from previous works (Li et al., 2019; Chi et al., 2021).

Results and discussion

Polysaccharide chemical characterization

The polysaccharide extraction of the green macroalga *Ulva fasciata* allowed a recovery of 17.5% dry weight (working fraction: U, Table S1), obtaining a colorless polysaccharide with light cotton aspect. The analysis by HPSEC revealed that the M_w of U polysaccharide was $2.12 \times 10^5 \text{ g mol}^{-1}$. The results of chemical analyses and monosaccharide composition can be found in Tables S1 and S2.

PVA:U solution for electrospinning

In the present work, aqueous systems with different PVA:U ratios were tested to finally select the PVA:U blend mass ratio 5:2 (PVA5U2) as the working system. This was based on the spinnable character of the blend and uniformity of the fibers (Figures S1 a-b). The system was characterized by rheological and surface tension measurements and ^1H NMR analysis.

Rheological and surface tension of PVA5U2 solution

The selection of the proper solvent during the formulation of spinnable mixtures, represent an essential condition to define the occurrence of spraying (formation of droplets) or spinning (production of fibers). This is because solvent physical characteristics exert a remarkable influence over important aspects associated to the electrospinning process, such as: the rheology of the mixture (Mejía Agüero et al., 2022).

In the pioneering work of Toskas et al. (2011), ulvan was mixed with boric acid/calcium chloride ($\text{H}_3\text{BO}_3:\text{CaCl}_2$) water solution to obtain a spinnable system. The solution was characterized as presenting a viscoelastic gel-like behavior ($G' > G''$). Due to the limited flow behavior of ulvan in this solvent, Toskas et al. (2011) introduced PVA to the mixture, to obtain a spinnable system. The authors noted the occurrence of rheological changes that favored the electrospinning process, where G'' dominated G' at low frequencies, characteristic of a viscoelastic-liquid behavior.

In the present work, the $\text{H}_3\text{BO}_3:\text{CaCl}_2$ water solution was replaced by ultrapure water, as previously used by Madany et al. (2021); leading to the formation of non-spinnable pure U aqueous solutions. The spherical like-shape conformation exhibited by pure ulvan in aqueous systems (Carvalho et al., 2020) limited the creation of sufficient entanglements (chains percolation), preventing jet formation as a hypothesis. As an alternative, the introduction of another polymer into ulvan systems, such as PVA could act by trapping ulvan, increasing the chain percolation and becoming suitable for electrospinning (Mejía Agüero et al., 2022).

As performed by Toskas et al. (2011) and Madany et al. (2021) the polymer selected in the present work was also PVA. However, the M_w of PVA, U/PVA ratio and the ulvan (chemical composition) contained in the system formulated

by Madany et al. (2021), were distinctive from those in the system formulated in the present work. As previously reported by Robic, Sassi, Dion, Lerat & Lahaye (2009), Kidgell et al. (2021) and Doderio et al. (2019), the molar mass, the polymers mass ratio in the mixture and the inherent characteristics of the polysaccharide used to form a system, will affect the solution rheology, and hence, the electrospinning process. Consequently, the aqueous system inherent characteristics used by Madany et al. (2021) will be different of the one used in the present work. These corresponded to two different ulvan colloidal aqueous systems.

Rheological measurements performed in the PVA5U2 system, U, and PVA solutions produced in this work, showed that the (G'') modulus was greater than (G') (Figure 1a-c, Figures S2a-c), indicating that these solutions exhibited liquid-like viscoelastic behavior (Sari-Chmayssem et al., 2019). Consequently, the substitution of $\text{H}_3\text{BO}_3:\text{CaCl}_2$ solution by ultrapure water during the fabrication of ulvan-based fibers, allow to overcome the drawback associated with gel formation, producing solutions with no measurable yield stress.

From the results above it is possible to note that G'' over G' is a necessary but not sufficient condition to guarantee the electrospinning of ulvan solutions. The viscosity and the viscoelastic properties will also define the spinnability of polymer solutions. Additionally, as observed in the Figure 1, a transitory network was observed at higher frequencies, and the relaxation time (τ), defined as $\tau=1/f$ when $G'=G''$, reduced 10 times when U was mixed with PVA. Another important observation is that τ is almost the same for U:PVA and pure PVA, demonstrating that the lower τ is associated to an improved relaxation of stored elastic stresses thought a rearrangement and conversion to viscous stresses.

Viscosity profile and thixotropic property were also evaluated in this work (Figure 1d). The result obtained for the first determination showed that the samples (U 2wt% solution, PVA 5wt% solution, and PVA5U2 system) exhibited the characteristic behavior of Newtonian and non-thixotropic fluids, since no significant hysteresis was observed. A considerable increase in the PVA5U2 viscosity was observed when compared with its two individual's components (U2wt% and PVA 5wt% solutions). This behavior has been previously correlated with the occurrence of intermolecular interactions, probably via hydrogen bonding (Shen & Hsieh, 2014).

The previous result contrasts with the one reported by Toskas et al. (2011) for the ulvan/ $\text{H}_3\text{BO}_3/\text{CaCl}_2$ system, in which a decrease of viscosity favored the electrospinning. This difference could be explained as a consequence of the distinct natures of the solvent systems nature used in each case, and the interaction effect between ulvan and the $\text{H}_3\text{BO}_3:\text{CaCl}_2$ solvent. The edge effect on the rheological behavior is presented in Figure S3.

Surface tension measurements performed for U (2 wt%), PVA (5 wt%) and PVA5U2 solutions, corresponded to: $66.75 + 0.4 \text{ mN.m}^{-1}$, $48.09 + 0.3 \text{ mN.m}^{-1}$ and $47.56 + 0.3 \text{ mN.m}^{-1}$, respectively. These results showed that the PVA5U2 blend exhibited a reduction in the surface tension when compared to the U solution, compatible with pure PVA 5 wt%. The surface tension decrease of PVA5U2 system is a consequence of the shrinking force decreasing, which contributes (among other factors) to improve the jet formation and promotes spinning

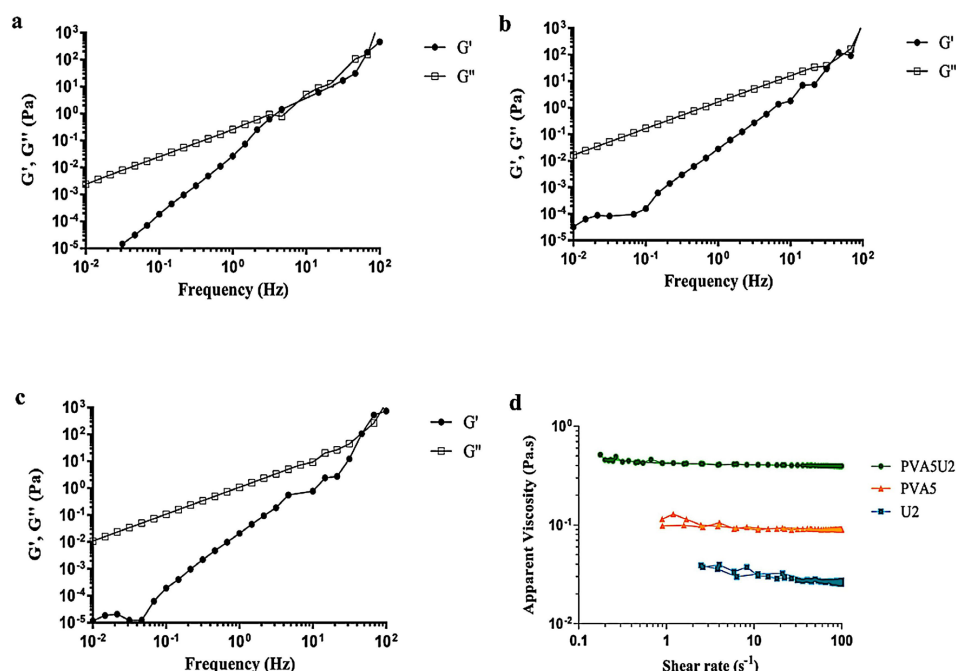


Figure 1. G' and G'' as a function of the frequency and shear stress at 20 °C for: (a) U 2 wt % solution, (b) 5 wt %, PVA solution and (c) mixture PVA5U2. Shear rate effect on the apparent viscosity of U 2wt% solution, PVA 5wt% solution and the PVA5U2 system, considering the thixotropic property at 20 °C (d).

(Rwei & Huang, 2012). As previously mentioned, a high surface tension induces bead formation, therefore, lower surface tensions are desirable to obtain continuous fibers with higher surface area (Williams et al., 2018; Fong et al., 1999).

The rheological and surface tension analyses performed in the PVA5U2, evidenced interesting characteristics for this system, attending the objectives set out in the present work. Behind the liquid-viscoelastic behavior which prevented the formation of a viscous gel, the non-thixotropic behavior of this system evidenced that the PVA5U2 system has a certain degree of elongation, which is desirable to prevent jet break under the effects of the electric forces applied during the electrospinning (Mata et al., 2022). Additionally, we observed that the surface tension of this system favored the electrospinning process using lower electric fields.

¹H NMR of PVA5U2 solution and its individual components

Spectroscopic analysis of PVA5U2 solution was performed considering the changes suffered in the embedded materials properties of a mixture, as previously reported (Kamoun et al., 2014). Aiming to describe the NMR spectroscopic characteristics of the U and PVA mixture, ¹H NMR analyses of the PVA5U2 system and of its individual components, U and PVA, were carried out and presented in the Figures 2, S4, and S5. Chemical assignments for U are shown in Table S3 and those for PVA (dissolved in D₂O and Me₂SO-*d*₆) are compared in Table S4.

The ¹H NMR analysis of PVA5U2 solution (Figure 2) showed various peaks also present in the spectrum of U solution

and all the characteristic ¹H peaks of PVA. The main ¹H chemical shifts of PVA5U2, U, and PVA solutions were assigned according to previous references (Table S5) (van der Velden & Beulen, 1982; Shaohua et al., 1990; Petit & Zhu, 1996; Lahaye & Robic, 2007; Lahaye, 1998; Lahaye et al., 1997, 1998; Carvalho et al., 2018; Aranha & Lucas, 2001; Amiya, 1994; Amiya et al., 1990).

The PVA5U2 spectrum (Figure 2) clearly shows two peaks at 4.85 and 4.65 ppm, the first one was attributed to the anomeric proton of α -L-rhamnose 3-sulfate linked to β -D-glucuronic acid, while the second resonance corresponds to the anomeric protons of β -D-glucuronic acid and β -D-xylose of U. Additional signals corresponding to the polysaccharide unit ring protons at 3.81-3.36 ppm, as well as the resonance at 1.32 ppm attributed to H-6 of α -L-Rhap of U were also observed in PVA5U2 mixture (Figure 2, Tables S3 and S5). In contrast with that, some U resonances, such as those of iduronic units at 3.68 (H-2) and 3.84 (H-3) ppm disappear in the PVA5U2 spectrum while others could be overlapped by the PVA signals. These results confirm the presence of both polymers in the PVA5U2 mixture. As a first approach, we consider that U anomeric signals at 5.18 and 4.91 ppm as well as ring proton resonances between 4.09-3.86 ppm could be overlapped by the methine PVA signals at 5.22-4.92 and 4.03 ppm, respectively. Besides, the considerable decrease in the peak intensity of α -L-Rhap H-6 (1.32 ppm) could indicate that rhamnose units interact with PVA. Further studies will be necessary aiming to describe all possible chemical interactions between U and PVA in aqueous system.

PVA5U2 nanofiber mat

The PVA5U2 mat behavior in aqueous systems must be considered in order to determine the potential uses of

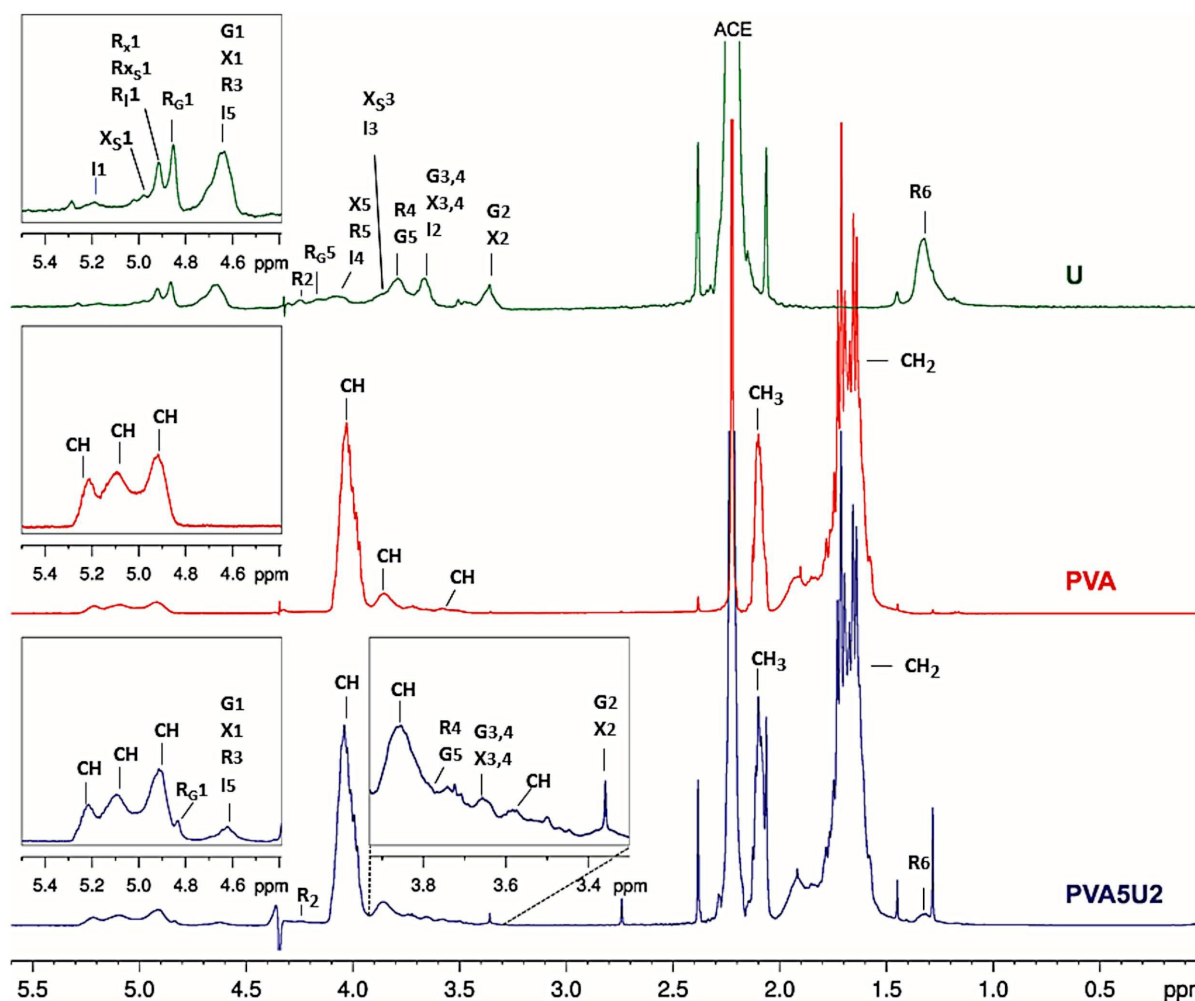


Figure 2. ^1H NMR spectra of PVA5U2, PVA, and U (solvent: D_2O , temperature: 70°C , ACE: acetone internal reference). Monosaccharide units of each U dyad (A_{35} , U_{35} , B_{35}) are represented as follows: R: rhamnose, G: glucuronic acid, X: xylose, I: iduronic acid unit. R_G , R_X , R_I represent rhamnose 3-sulfate linked to glucuronic acid, xylose, or iduronic acid, respectively. Subscripted numbers represent the corresponding hydrogen. PVA: CH_3 , CH_2 , and CH correspond to the methyl, methylene, and methine groups of PVA, respectively.

ulvan-PVA nanofibers. Bearing in mind biotechnological applications, it would be desirable that the PVA5U2 nanofiber mat should be stable in aqueous medium. However, as it would be expected from the PVA5U2 nanofiber mat composition (two water-soluble polymers), the U-based mat produced in this work readily solubilized upon contacting with water (Figure 3 (aiii)).

To face the drawback of polysaccharide-based nanofibers water-solubility, some authors have used chemical crosslinking to stabilize this type of biomaterials in water (Morelli & Chiellini, 2010; Alves et al., 2012). Nevertheless, attending to the objectives of this research, an alternative crosslinking method was evaluated to avoid the instant dissolution of PVA5U2 nanofiber mat upon contacting with water.

As an alternative crosslinking method, thermal crosslinking has been effectively applied to PVA and PVA/polysaccharide mixture mats (Pelipenko et al., 2013; Lubambo et al., 2015). Considering these previous results, the thermal crosslinking of PVA5U2 mat was evaluated following the method employed by Pelipenko et al. (2013).

After the thermal treatment (160°C for 30 min), the PVA5U2 crosslinked mat was tested by submerging it in purified water (Figure 3(b)), obtaining a thin mat with a jelly foil aspect that showed to be stable after heat drying, exhibiting a moistening resistant behavior. Despite it, a fast increase in its gel consistency was observed after ten minutes of immersion in water; acquiring a softer appearance up to its progressive and complete dissolution.

As a second approach to stabilize the mat using only dry heat, an increase in the crosslinking temperature was also evaluated (at 170°C or 180°C). The results showed a close similar behavior between the mat heated at 170°C (30 min) and the one treated at 160°C (30 min). However, an improved stability was exhibited for the mat heated at 180°C for 30 min, despite the observation of a decrease in its firmness over the time. Our strategy using a higher temperature (180°C) was combined with a longer time (60 min) treatment, resulting in a mat exhibiting good stability during the first 3 hours of immersion in water (Figure 4). Consequently, the water stability of the crosslinked PVA5U2 mat was enhanced by increasing the crosslinking temperature and time of treatment.

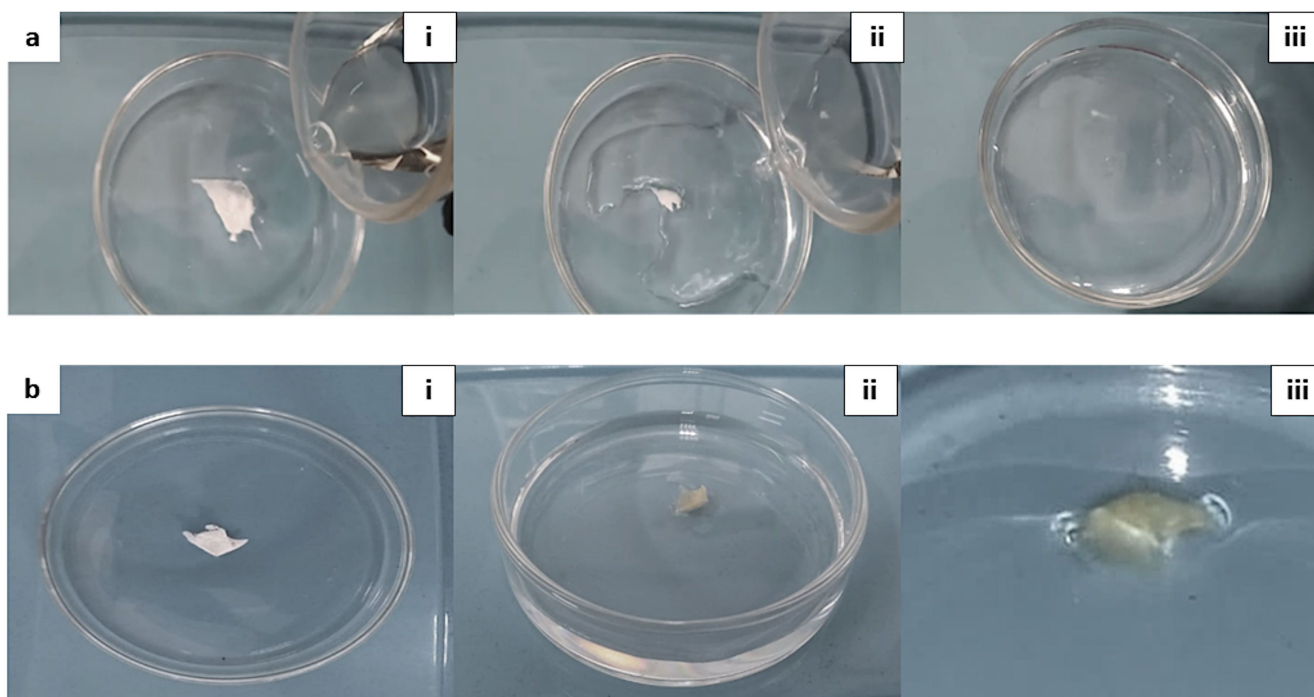


Figure 3. (a) PVA5U2 nanofiber mat and (b) thermally-crosslinked (160 °C for 30 min) PVA5U2 nanofiber mat: (i) as deposited, (ii) in purified water, (iii) after 10 min submerged in distilled water.

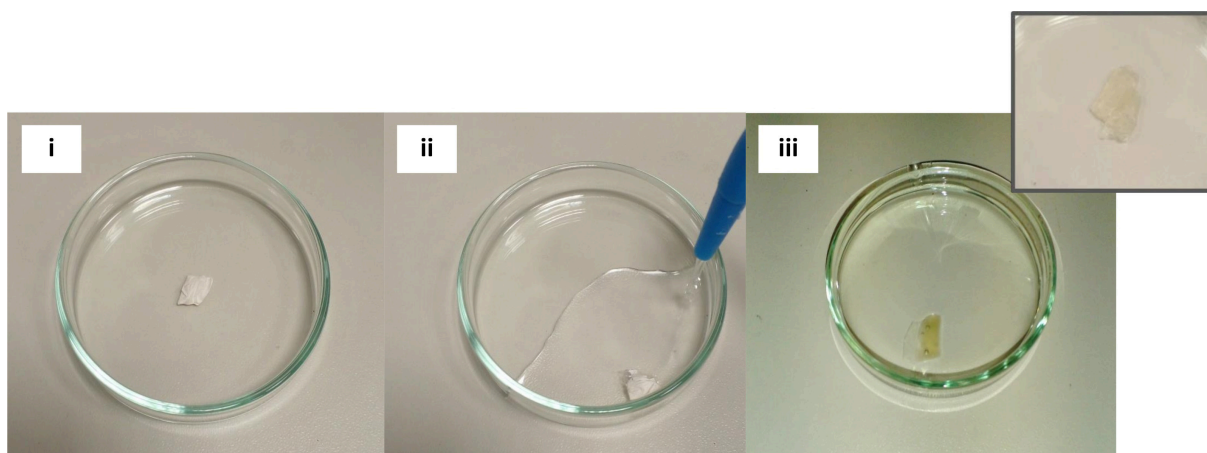


Figure 4. PVA5U2 thermally-crosslinked nanofiber mat (180 °C for 60 min): (i) after deposited and treated, (ii) in distilled water, (iii) after 10 min submersed in distilled water.

PVA5U2 nanofiber mat scanning electron microscopy (SEM) analyses

As a first approach to describe the physical morphology of this novel biomaterial, the crosslinked PVA5U2 mat was examined by SEM (Figure 5). Firstly, the microscopic analyses were performed before and after the thermal treatment. Figure 5a corresponds to the native PVA5U2 nanofibers SEM micrograph, exhibiting a random arrangement of elongated and uniform fibers with mean diameter of 144 ± 33 nm with few enlargements up to 355 nm. SEM analysis of the crosslinked PVA5U2 mat exhibited nanofibers with mean diameter of

160 ± 42 nm with few enlargements up to 380 nm, without significant changes in the morphology (Figure 5b).

In this work, the diameter of the produced fiber was bigger than reported by Madany et al. (2021). Some aspects responsible for this difference were the higher ulvan mass used in the mixture prepared by Madany et al. (2021), as well as, the higher voltage (24 kV) used by them during the electrospinning process. Toskas et al. (2011) stated that the electrospinning of aqueous solutions demands high voltages because of the high surface tension of water. In the present work, surface tension measurements of the PVA:U aqueous blends evidenced a drop in the surface tension values ($47.56 \pm$

$0.3 \text{ mN}\cdot\text{m}^{-1}$) with respect to both the water surface tension ($72.8 \text{ mN}\cdot\text{m}^{-1}$) and the U solutions ($66.75 \pm 0.4 \text{ mN}\cdot\text{m}^{-1}$). As a consequence, in the present work, the electrospinning of the PVA:U solutions was performed at lower voltages ($17 \pm 1 \text{ kV}$) than those used in previous studies (Toskas et al., 2011; Madany et al., 2021).

The crosslinked PVA5U2 ($180^\circ\text{C}/60 \text{ min}$) was examined at the end of each water immersion time, evidencing that nanofibers were conserved in the mat. From the results obtained, nanofibers with an increase in the mean diameter were observed, showing $176 \pm 35 \text{ nm}$ (after 30 min immersion), $172 \pm 32 \text{ nm}$ (after 60 min immersion), $165 \pm 46 \text{ nm}$ (after 120 min immersion), and $186 \pm 52 \text{ nm}$ (after 180 min immersion) (Figure 6). Important variations in the mean diameter of the fibers were not observed during

the first two hours of immersion. An increase in the mean diameter of about 30% from the native nanofibers and 16% from the crosslinked fibers was observed after 180 min of immersion.

From the results obtained in this research, interactions between U and PVA were detected by NMR, FTIR, and rheological analyses. As determined by ATR-FTIR (to be discussed later), hydrogen bonding seems to play an important role in the PVA5U2 mat conservation. Hydrogen bonds are able to undergo reversible changes under different solution environments, such as pH, temperature, solvent, and ion type and strength (Qi et al., 2021). Then, as would be expected, the thermally-crosslinked PVA5U2 mat was not stabilized by the permanent covalent bonds that would be characteristic in a chemical crosslinking (Qi et al., 2021).

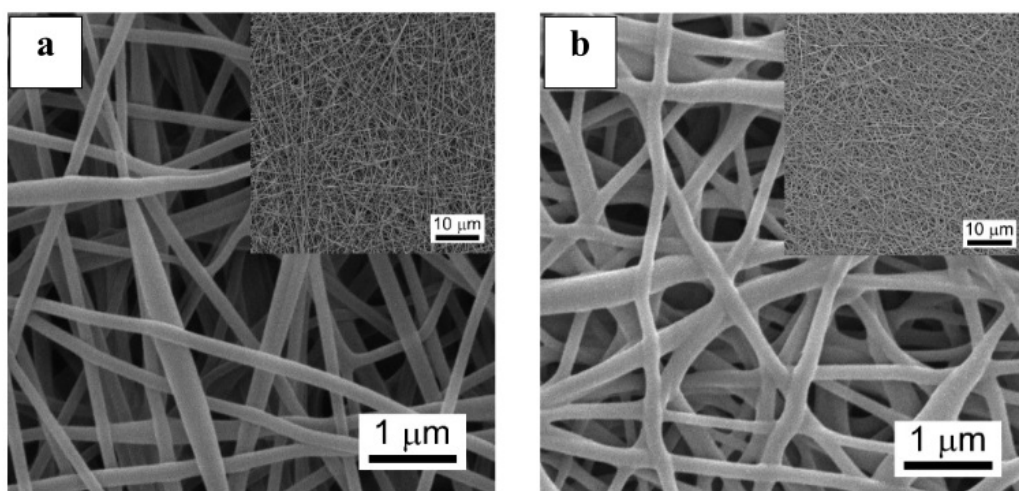


Figure 5. Scanning electron microscopy analysis of (a) PVA5U2 nanofiber mat (b) thermally-crosslinked nanofiber mat.

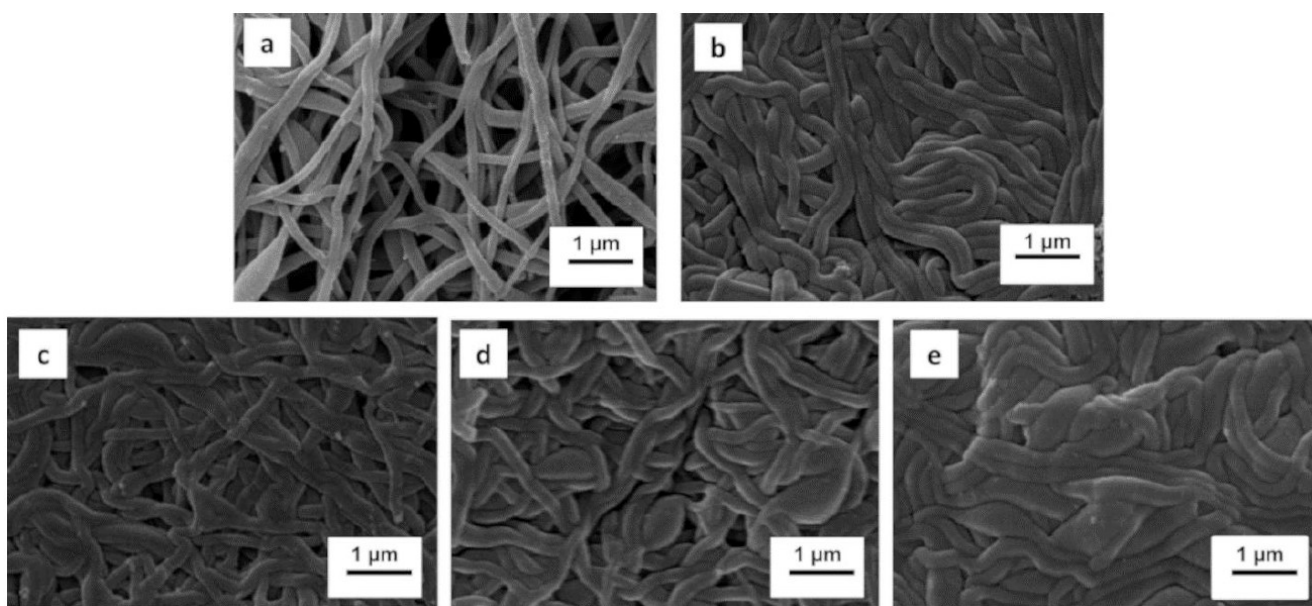


Figure 6. Scanning electron microscopy analysis of PVA5U2 nanofiber mat. (a) thermally-crosslinked nanofibers mat, (b) after 30 min, (c) 60 min, (d) 120 min, (e) 180 min of water immersion.

Based on what was previously mentioned, the PVA5U2 mat appears as an interesting platform for post spinning surface crosslinking events and different application purposes.

ATR-FTIR analysis of PVA5U2 nanofiber mat

The PVA5U2 nanofiber mat ATR-FTIR spectrum was compared with those of U and PVA (Figure 7), and their absorption bands attributed in agreement with previous reports (Zhang et al., 2010; Thu et al., 2016; Robic, Bertrand, Sassi, Lerat, & Lahaye (2009); Raveendran et al., 2013; Krimm et al., 1956; Jaulneau et al., 2010).

The PVA5U2 FTIR spectrum presented a reduction in the intensity of the following absorption bands of both U and PVA (Figure S6, S7, S8 and S9): the asymmetrical stretching vibration of U $-\text{COO}^-$ groups (1600 cm^{-1}) and the PVA bands corresponding to: OH (3303 cm^{-1}), CH_2 (2939 and 2906 cm^{-1}), the carbonyl from carboxylic acid groups (1734 cm^{-1}) and oxygen associated to the non-hydrolyzed acetate (1714 cm^{-1}) (Zhang et al., 2010) and the CH_2 and CH-OH groups (1376 and 1325 cm^{-1}). The variations observed in these bands suggested that these groups could be taking part in chemical interactions established within the PVA5U2 nanofiber mat.

Comparison of PVA5U2 mat spectrum with that obtained by Toskas et al. (2011) showed differences in the band corresponding to the U $-\text{COO}^-$ groups. While Toskas et al. (2011) reported a shift (from 1620 to 1713 cm^{-1}), in the present study the $-\text{COO}^-$ band is in the same range than that observed in the U spectrum (1608 - 1600 cm^{-1}) (Figure S6 and S7). Furthermore, the band at 1713 cm^{-1} , referred by Toskas et al. (2011) as a shift for the original $-\text{COO}^-$ band, was observed at the same position in both PVA5U2 and PVA spectra (Figures S8 and S9). For this reason, in the present research, the band at 1714 cm^{-1} was attributed to the PVA non-hydrolyzed acetate groups (Krimm et al., 1956). Additionally, it was possible to observe both bands (1608 and 1712 cm^{-1}) in the PVA5U2 mat spectrum with reduced intensity in respect to the reference spectra (Figures S6, S7, S8, S9). The reduction observed in the $-\text{COO}^-$ FTIR band together with the ^1H NMR results suggest that the PVA-U interactions could mainly occur

through the polysaccharide uronic acid units. The differences observed between the present study and the one carried out by Toskas et al. (2011) can be attributed to the solvent system utilized in each case, while the latter authors used $\text{H}_3\text{BO}_3/\text{CaCl}_2$ aqueous solution, the current research used only ultrapure water.

Increases in the intensities of FTIR bands at 2939 cm^{-1} (stretching of CH) and 1420 cm^{-1} (stretching vibration of $-\text{COO}^-$) were observed in PVA5U2 when compared to U spectrum (Figures 7, S6, and S7). These increases could be consequence of the overlapping of bands attributed to PVA CH_2 groups (Figure S8) that are not taking part in the polymer interactions. Moreover, the peak at 1244 cm^{-1} , in the region assigned to the wagging vibration of CH PVA groups, overlaps the stretching vibration band of U sulfate groups (S-O, 1217 cm^{-1}), exhibiting a similar behavior than that observed for the band at 842 cm^{-1} (Figure S6 (b)) that corresponds to the overlapping of $-\text{COS}$ bending vibration in axial position of U sulfate groups (847 cm^{-1}) and C-C stretching vibration band of PVA (at 833 cm^{-1}).

Finally, in the region between 1100 and 900 cm^{-1} of PVA5U2 mat spectrum a broad and intense absorption band centered at 1050 - 1029 cm^{-1} with shoulders at 1084 and 985 cm^{-1} was observed (Figure 7 and S6 (b)). When compared with the PVA and U spectra, a reduction in intensity can be observed in those bands attributed to stretching vibration of PVA $-\text{CO}$ (1084 cm^{-1}) and the stretching vibration of C-O-C of glycosidic U linkages (979 cm^{-1}), in parallel with an increase in the two central bands intensity, attributed to the stretching vibration of C-O (1050 cm^{-1}) of U (Figure S6 and S7), and the band at 1029 cm^{-1} attributed to an overlap of sugar ring vibration absorption bands with C-O-C glycosidic bonds and stretching vibration of C-OH of U and C-H₂ of PVA (Figures S7 and S8).

Our results exhibit similarities with those reported by Rynkowska et al. (2019) who characterized a chemically/thermally crosslinked PVA-based membrane, using sulfosuccinic acid (SSA), a chemical compound that presents $-\text{COOH}$ and $-\text{SO}_3\text{H}$ groups in its structure. Rynkowska et al. (2019) stated that PVA crosslinked by esterification between PVA $-\text{OH}$ groups and SSA $-\text{COOH}$ groups. In agreement with it, we also postulated that the $-\text{COO}^-$ groups of the polysaccharide may play an important role in the interactions between U and PVA. The participation of PVA $-\text{OH}$ groups (by hydrogen bond interactions) was justified by Rynkowska et al. (2019) for the significant decrease observed in the PVA $-\text{OH}$ group intensity, also observed in the PVA5U2 spectrum.

ATR-FTIR analysis of thermally-crosslinked PVA5U2 nanofiber mat before and after water immersion

After thermal crosslinking ($180^\circ\text{C}/60\text{ min}$), the PVA5U2 nanofiber mat FTIR spectrum exhibited the following absorption bands: 791 , 846 , 986 , 1027 , 1046 , 1087 , 1245 , 1326 , 1374 , 1417 , 1612 , 1716 , 1731 , 2915 , 2937 , and 3325 cm^{-1} (Figure 8a). Absorption bands at 791 , 846 , 986 , 1027 , 1245 , 1417 , and 1622 cm^{-1} were attributed to U groups (Figure S6), while those bands at 1087 , 1326 , 1374 , 1716 , 1731 , 2915 cm^{-1} were attributed to PVA (Figure S8a). Bands presented by U and PVA were observed at 2937 and 3325 cm^{-1} .

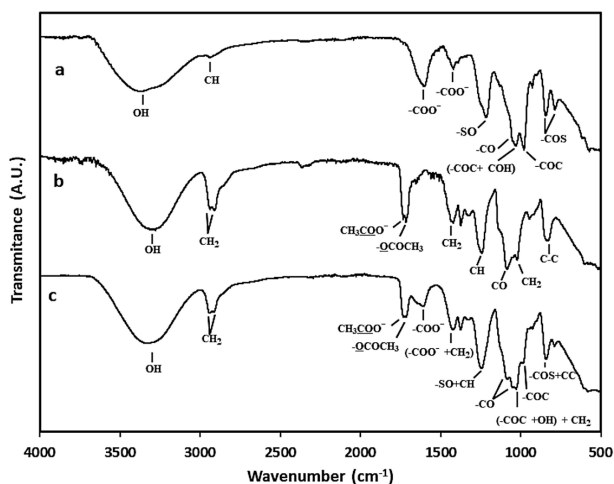


Figure 7. ATR-FTIR spectra of: (a) U, (b) PVA powder, and (c) PVA5U2 mat

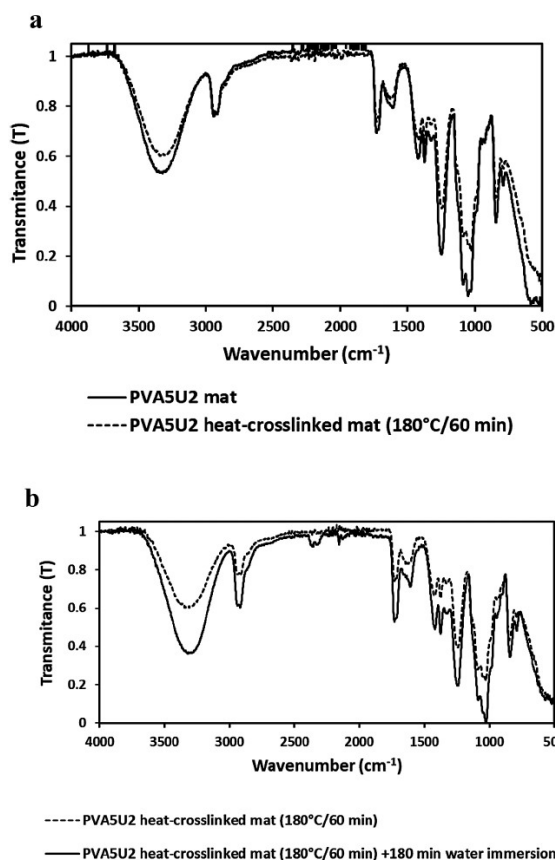


Figure 8. Comparison of ATR-FTIR spectra of: (a) PVA5U2 mat and PVA5U2 thermally-crosslinked mat, (b) PVA5U2 thermally-crosslinked mat before and after 180 min of water immersion.

The crosslinked mat exhibited the same bands observed in the original nanofiber mat as shown in Figure 8a.

Variations in the intensity of the crosslinked PVA5U2 mat FTIR bands compared with those of the native PVA5U2 were observed. A decrease in the intensity of the peaks depicted at 3325, 1731, 1716, 1622, 1417, 1374, 1326, 1245, 1087, 1027 986, 846, and 791 cm^{-1} were observed in the crosslinked PVA5U2 bands. These results clearly show that the thermal treatment does not compromise the polysaccharide functional groups present in the original PVA5U2 nanofiber mat.

After 180 min of water immersion, the ATR-FTIR spectrum of PVA5U2 crosslinked mat (180 °C for 60 min) exhibited the same absorption bands showed before immersion (Figure 8b).

ATR-FTIR analysis of PVA5U2 crosslinked mat after impregnation with a ferric chloride solution

Changes in the FTIR bands of crosslinked PVA5U2 mat functional groups were identified after impregnation with a ferric chloride solution (Figure 9). Firstly, the band depicted at 3325 cm^{-1} (stretching of OH) showed a lower intensity and narrow shape when compared with the band observed in the PVA5U2 crosslinked mat spectrum. In addition to it, the band at 1612 cm^{-1} , attributed to the carboxyl group of U showed a shift to 1652 cm^{-1} , and a decrease in its intensity; while the band at 1245 cm^{-1} in the region assigned to the wagging

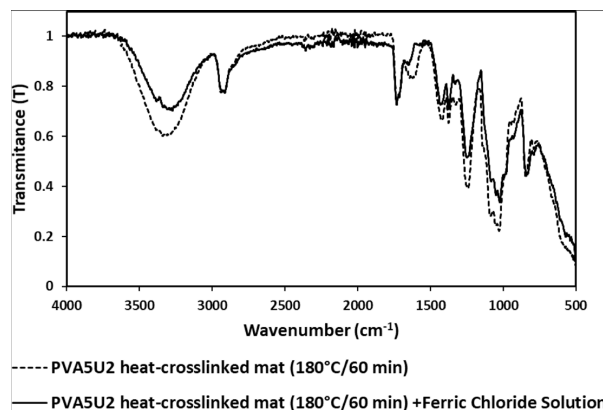


Figure 9. Comparison of ATR-FTIR spectra of PVA5U2 thermally-crosslinked mat and PVA5U2 thermally-crosslinked mat after impregnation with a ferric chloride solution.

Table 1. Swelling degree and dissolution degree of the PVA5U2 mat.

Immersion time (min)	SD (%)	Dissolution degree (%)
10	475.2 ± 17.5	11.9 ± 2.8
30	479.4 ± 41.6	14.5 ± 1.8
60	444.4 ± 30.8	18.4 ± 2.6
120	444.8 ± 36.2	22.6 ± 4.9
180	437.6 ± 44.8	28.3 ± 4.7

SD: mass swelling degree. The water uptake was calculated from the mass gain between the dried membrane and the membrane equilibrated in water.

vibration of CH from PVA overlaps the stretching vibration band of U sulfate groups, showed an increase in its intensity.

We assume that these results show the interactions between the Fe metal ion with the hydroxyl, carboxyl and sulfate groups involved in the PVA5U2 mat structure. These variations are similar to those reported by Li et al. (2019) for an ulvan derivative complexed with Fe(III) and the results obtained by Chi et al. (2021) who investigated the metal ion binding properties of *Ulva clathrata*. They reported that the hydroxyl groups on the ulvan chain, were the main functional groups participating in the adsorption of metal ions. In the present work, the bands at 1087, 1027, and 966 cm^{-1} (attributed to PVA -CO, the sugar ring vibration overlapping with C-O-C glycosidic bonds and C-OH of U, and the C-O-C stretching glycosidic bond of U) showed modifications in shape indicating that these groups could be participating in the interactions.

Swelling degree and dissolution degree of the PVA5U2 mat

The swelling behavior and dissolution rate of PVA5U2 mat (treated at 180 °C for 60 min) were evaluated at the end of each water immersion time. The results are shown in the Table 1.

The PVA5U2 mat swelling during the first hour was similar to the results of the immersion of an ionically crosslinked scaffold reported by other authors (Gajaria et al., 2020). The swelling percentages of the ulvan-calcium scaffold previously reported were: 405.33% \pm 39.50% (after 15 min of immersion), 439.17% \pm 22.10% (30 min), 466.27% \pm 17.30% (1 h), and 502.61% \pm 8.70% (at the end of 24 h).

The crosslinked PVA5U2 nanofiber mat exhibits important attributes for different applications (currently under investigation), envisaging studies in which the interaction with water-soluble elements is desirable (Webster et al., 1997; Santos et al., 2014; Persano et al., 2013; Mahinroosta et al., 2018). The chelating capacity of PVA5U2 mat as an iron-ligand, turns it out as suitable candidate to produce an easily degradable smart food-film for supplemented foods. Additionally, the swelling behavior exhibited by the PVA5U2 mat during the first hours of immersion in water, also shows it as an ideal candidate to produce wound healing biomaterials.

The strategy of using thermal crosslinking to stabilize the PVA5U2 mat against water impregnation created a smart and versatile platform that meets one of the scientific community focuses, the production of physical (or reversible) gels in which cross-linkers removal is unnecessary (Mahinroosta et al., 2018).

Conclusion

In this work, bead-free nanofibers from PVA/U aqueous system were produced, exhibiting an average diameter of 144 \pm 33 nm. Interactions between the seaweed sulfated polysaccharide and synthetic polymer in the PVA5U2 system were confirmed by ¹H NMR, ATR-FTIR, and rheological analyses. The ATR-FTIR and ¹H NMR results suggested that the uronic acid -COO⁻ groups present in U could be the main responsible for these interactions, which highlights the importance of the ulvan composition in the production of this kind of biomaterial. A considerable reduction of surface tension was observed in the PVA5U2 solution in comparison to U solution. The addition of PVA makes possible the spinning at lower voltage (17 \pm 1 kV) when compared to previous works. The reduction in the working voltage represents an important advantage during the fiber formation. The seaweed-derived biomaterial formed by two water-soluble polymers became water-resistant after thermal crosslinking. To the best of our knowledge, this is the first successful approach to stabilize an ulvan-based electrospun mat by a physical method. No significant changes in both, nanofiber chemical composition and morphology were observed after thermal crosslinking. From a biotechnological point of view, interesting aspects can be highlighted in this novel nanofiber mat, among which can be mentioned the presence of ionic functional groups (sulfate and carboxylic groups), water-resistant properties, and a fully biodegradable low-cost composition. Finally, considering the previous background, it is possible to conclude that the thermally-crosslinked PVA5U2 nanofiber mat corresponds to a versatile biomaterial, available for further chemical modifications and therefore functionalization.

Conflict of interests

The authors state no conflict of interest.

Funding: CKS, RAF, MRD, and MDN are Research Members of CNPq. This work was supported by the National Research Council of Brazil (CNPq, Universal Call: 462414/2014-0 and 422579/2021-1 and PQ-CNPq: 306568/2018-7) and Coordenação de Aperfeiçoamento de Pessoal de Nível Superior (CAPES, Brazil) - Finance Code 001 and PrInt/CAPES.

Acknowledgements

The authors wish to thank CME-UFPR for the microscopic analyses (specially to Dr. Ney Mattoso, Msc. Eduardo Tusset and MSc./CME member Rosangela B. Freitas for their invaluable technical assistance), UFPR-NMR Center for the NMR analyses, and CEB-UFPR for the FTIR analyses (specially to PhD student Alexander Cobre and Phar. Raquel de Oliveira). To Drs. Mariana Carvalho, Romelly Rojas, Keylla L. Miscchiatti and Dr. Lauri Alves. L.E.M.A. Thanks PAEC (Programa de Alianzas para la Educación y la Capacitación), OEA/GCUB (Organización de los Estados Americanos/GrupoCoimbra de Universidades Brasileiras) and CAPES by a doctoral scholarship, also thanks a doctoral leave by Fac. Ciencias, Universidad Central de Venezuela (UCV), and thanks Jesi Mejia A. for her assistance during the development of this manuscript.

References

- Alves, A., Pinho, E., Neves, N., Sousa, R., & Reis, R. (2012). Processing ulvan into 2D structures: Cross-linked ulvan membranes as new biomaterials for drug delivery applications. *International Journal of Pharmaceutics*, 426(1-2), 76-81. <http://dx.doi.org/10.1016/j.ijpharm.2012.01.021>. PMID:22281048.
- Alves, A., Sousa, R., & Reis, R. (2013). A practical perspective on ulvan extracted from green algae. *Journal of Applied Phycology*, 25(2), 407-424. <http://dx.doi.org/10.1007/s10811-012-9875-4>.
- Amiya, S. (1994). A nuclear magnetic resonance study of the microstructure of poly(vinyl alcohol). In K. P. Ghiggino (Ed.), *Progress In Pacific Polymer Science 3: Proceedings of the Third Pacific Polymer Conference*. (1st ed., pp. 367-379). Springer. <https://doi.org/10.1007/978-3-642-78759-1>
- Amiya, S., Tsuchiya, R., Qian, R., & Nakajima, A. (1990). The study of imcrostructures of poly(vinyl alcohol) by NMR. *Pure and Applied Chemistry*, 62(11), 2139-2146. <http://dx.doi.org/10.1351/pac199062112139>.
- Amjadi, S., Almasi, H., Ghorbani, M., & Ramazani, S. (2020). Reinforced ZnONPs/ rosemary essential oil-incorporated zein electrospun nanofibers by κ-carrageenan. *Carbohydrate Polymers*, 232, 115800. <http://dx.doi.org/10.1016/j.carbpol.2019.115800>. PMID:31952599.
- Anderson, M. A., & Stone, B. A. (1985). A radiochemical approach to the determination of carboxylic acid groups in polysaccharides. *Carbohydrate Polymers*, 5(2), 115-129. [http://dx.doi.org/10.1016/0144-8617\(85\)90029-3](http://dx.doi.org/10.1016/0144-8617(85)90029-3).
- Aranha, I. B., & Lucas, E. F. (2001). Poli(álcool vinílico) modificado com cadeias hidrocarbônicas: Avaliação do balanço hidrófilo/lipófilo. *Polímeros: Ciência e Tecnologia*, 11(4), 174-181. <http://dx.doi.org/10.1590/S0104-14282001000400007>.
- Barnes, C. P., Sell, S., Boland, E., Simpson, D., & Bowlin, G. (2007). Nanofiber technology: Designing the next generation of tissue

- engineering scaffolds. *Advanced Drug Delivery Reviews*, 59(14), 1413-1433. <http://dx.doi.org/10.1016/j.addr.2007.04.022>. PMID:17916396.
- Bhardwaj, N., & Kundu, S. C. (2010). Electrospinning: A fascinating fiber fabrication technique. *Biotechnology Advances*, 28(3), 325-347. <http://dx.doi.org/10.1016/j.biotechadv.2010.01.004>. PMID:20100560.
- Carpita, N., & Shea, E. (1990). Linkage structure of carbohydrates by gas chromatography-mass spectrometry (GC-MS) of partially mutilated alditol acetates. In G. D. Biermann & C. J. McGinnins (Eds.), *Analysis of carbohydrates by GLC and MS of carbohydrates by GLC and MS* (2nd ed., pp. 157-216). CRC Press.
- Carvalho, M. M., Freitas, R. A., Ducatti, D. R. B., Ferreira, L. G., Gonçalves, A. G., Colodi, F. G., Mazepa, E., Aranha, E. M., Nosedá, M. D., & Duarte, M. E. R. (2018). Modification of ulvans via periodate-chlorite oxidation: Chemical characterization and anticoagulant activity. *Carbohydrate Polymers*, 197, 631-640. <http://dx.doi.org/10.1016/j.carbpol.2018.06.041>. PMID:30007656.
- Carvalho, M. M., Nosedá, M. D., Dallagnol, J. C. C., Ferreira, L. G., Ducatti, D. R. B., Gonçalves, A. G., Freitas, R. A., & Duarte, M. E. R. (2020). Conformational analysis of ulvans from *Ulva fasciata* and their anticoagulant polycarboxylic derivatives. *International Journal of Biological Macromolecules*, 162, 599-608. <http://dx.doi.org/10.1016/j.ijbiomac.2020.06.146>. PMID:32565303.
- Cassolato, J. E. F., Nosedá, M. D., Pujol, C. A., Pellizzari, F. M., Damonte, E. B., & Duarte, M. E. R. (2008). Chemical structure and antiviral activity of the sulfated heterorhamnan isolated from the green seaweed *Gayralia oxysperma*. *Carbohydrate Research*, 343(18), 3085-3095. <http://dx.doi.org/10.1016/j.carres.2008.09.014>. PMID:18845298.
- Chi, Y., Li, H., Fan, L., Du, C., Zhang, J., Guan, H., Wang, P., & Li, R. (2021). Metal-ion-binding properties of ulvan extracted from *Ulva clathrata* and structural characterization of its complexes. *Carbohydrate Polymers*, 272(5), 118508. <http://dx.doi.org/10.1016/j.carbpol.2021.118508>. PMID:34420753.
- Colodi, F. G., Ducatti, D. R. B., Nosedá, M. D., de Carvalho, M. M., Winnischofer, S. M. B., & Duarte, M. E. R. (2021). Semi-synthesis of hybrid ulvan-kappa-carrabiose polysaccharides and evaluation of their cytotoxic and anticoagulant effects. *Carbohydrate Polymers*, 267, 118161. <http://dx.doi.org/10.1016/j.carbpol.2021.118161>. PMID:34119135.
- Cunha, L., & Grenha, A. (2016). Sulfated seaweed polysaccharides as multifunctional materials in drug delivery applications. *Marine Drugs*, 14(3), 1-41. <http://dx.doi.org/10.3390/md14030042>. PMID:26927134.
- Daemi, H., Mashayekhi, M., & Modaress, M. P. (2018). Facile fabrication of sulfated alginate electrospun nanofibers. *Carbohydrate Polymers*, 198, 481-485. <http://dx.doi.org/10.1016/j.carbpol.2018.06.105>. PMID:30093025.
- Doderó, A., Vicini, S., Alloisio, M., & Castellano, M. (2019). Sodium alginate solutions: Correlation between rheological properties and spinnability. *Journal of Materials Science*, 54(10), 8034-8046. <http://dx.doi.org/10.1007/s10853-019-03446-3>.
- Dodgson, K. S., & Price, R. G. (1962). A note on the determination of the ester sulphate content of sulphated polysaccharides. *The Biochemical Journal*, 84(1), 106-110. <http://dx.doi.org/10.1042/bj0840106>. PMID:13886865.
- Dubois, M., Gilles, K. A., Hamilton, J. K., Rebers, P. A., & Smith, F. (1956). Colorimetric method for determination of sugars and related substances. *Analytical Chemistry*, 28(3), 350-356. <http://dx.doi.org/10.1021/ac60111a017>.
- Filiseti-Cozzi, T. M. C. C., & Carpita, N. C. (1991). Measurement of uronic acids without interference from neutral sugars. *Analytical Biochemistry*, 197(1), 157-162. [http://dx.doi.org/10.1016/0003-2697\(91\)90372-Z](http://dx.doi.org/10.1016/0003-2697(91)90372-Z). PMID:1952059.
- Fong, H., Chun, I., & Reneker, D. H. (1999). Beaded nanofibers formed during electrospinning. *Polymer*, 40(16), 4585-4592. [http://dx.doi.org/10.1016/S0032-3861\(99\)00068-3](http://dx.doi.org/10.1016/S0032-3861(99)00068-3).
- Gajaria, T. K., Bhatt, H., Khandelwal, A., Vasu, V. T., Reddy, C. R. K., & Lakshmi, D. S. (2020). A facile chemical cross-linking approach toward the fabrication of a sustainable porous ulvan scaffold. *Bioactive and Compatible Polymers/Lymers*, 35(4-5), 301-313. <http://dx.doi.org/10.1177/0883911520939986>.
- Gibson, P., Schreuder-gibson, H., & Rivin, D. (2001). Transport properties of porous membranes based on electrospun nanofibers. *Colloids and Surfaces. A, Physicochemical and Engineering Aspects*, 187-188, 469-481. [http://dx.doi.org/10.1016/S0927-7757\(01\)00616-1](http://dx.doi.org/10.1016/S0927-7757(01)00616-1).
- Greiner, A., & Wendorff, J. H. (2007). Electrospinning: A fascinating method for the preparation of ultrathin fibers. *Angewandte Chemie International Edition*, 46(30), 5670-5703. <http://dx.doi.org/10.1002/anie.200604646>. PMID:17585397.
- Hwang, P. A., Chen, H. Y., Chang, J. S., & Hsu, F. Y. (2023). Electrospun nanofiber composite mat based on ulvan for wound dressing applications. *International Journal of Biological Macromolecules*, 253(Pt 1), 126646. <http://dx.doi.org/10.1016/j.ijbiomac.2023.126646>. PMID:37659492.
- Jaulneau, V., Lafitte, C., Jacquet, C., Fournier, S., Salamagne, S., Briand, X., Esquerré-Tugayé, M. T., & Dumas, B. (2010). Ulvan, a sulfated polysaccharide from green algae, activates plant immunity through the jasmonic acid signaling pathway. *Journal of Biomedicine & Biotechnology*, 2010, 525291. <http://dx.doi.org/10.1155/2010/525291>. PMID:20445752.
- Jesus Raposo, M. F., Morais, A. M., & Costa de Morais, R. M. (2015). Marine polysaccharides from algae with potential biomedical applications. *Marine Drugs*, 13(5), 2967-3028. <http://dx.doi.org/10.3390/md13052967>. PMID:25988519.
- Kamoun, E. A., Chen, X., Mohy Eldin, M. S., & Kenawy, E. S. (2014). Crosslinked poly(vinyl alcohol) hydrogels for wound dressing applications : A review of remarkably blended polymers. *Arabian Journal of Chemistry*, 8(1), 1-14. <http://dx.doi.org/10.1016/j.arabjoc.2014.07.005>.
- Kidgell, J. T., Carnachan, S. M., Magnusson, M., Lawton, R. J., Sims, I. M., Hinkley, S. F. R., De Nys, R., & Glasson, C. R. K. (2021). Are all ulvans equal? A comparative assessment of the chemical and gelling properties of ulvan from blade and filamentous *Ulva*. *Carbohydrate Polymers*, 264, 525291. <http://dx.doi.org/10.1016/j.carbpol.2021.118010>. PMID:33910714.
- Kikionis, S., Ioannou, E., Toskas, G., & Roussis, V. (2015). Electrospun biocomposite nanofibers of ulvan/PCL and ulvan/PEO. *Journal of Applied Polymer Science*, 132(26), 1-5. <http://dx.doi.org/10.1002/app.42153>.
- Kikionis, S., Koromvoki, M., Tagka, A., Polichronaki, E., Stratigos, A., Panagiotopoulos, A., Kyritsi, A., Karalis, V., Vitsos, A., Rallis, M., Ioannou, E., & Roussis, V. (2022). Ulvan-based nanofibrous patches enhance wound healing of skin trauma resulting from cryosurgical treatment of keloids. *Marine Drugs*, 20(9), 551. <http://dx.doi.org/10.3390/md20090551>. PMID:36135740.
- Krimm, S., Liang, C. Y., & Sutherland, G. B. M. (1956). Infrared spectra of high polymers. *Polyvinyl Alcohol*, 22(101), 227-247.
- Lahaye, M. (1998). NMR spectroscopic characterisation of oligosaccharides from two *Ulva rigida* ulvan samples (Ulvales, Chlorophyta) degraded by a lyase. *Carbohydrate Research*, 314(1-2), 1-12. [http://dx.doi.org/10.1016/S0008-6215\(98\)00293-6](http://dx.doi.org/10.1016/S0008-6215(98)00293-6). PMID:10230036.
- Lahaye, M., & Robic, A. (2007). Structure and functional properties of ulvan, a polysaccharide from green seaweeds. *Biomacromolecules*, 8(6), 1765-1774. <http://dx.doi.org/10.1021/bm061185q>. PMID:17458931.
- Lahaye, M., Brunel, M., & Bonnin, E. (1997). Fine chemical structure analysis of oligosaccharides produced by an ulvan-lyase degradation of the water-soluble cell-wall polysaccharides from *Ulva* sp. (Ulvales, Chlorophyta). *Carbohydrate Research*, 304(3-4), 325-333. [http://dx.doi.org/10.1016/S0008-6215\(97\)00270-X](http://dx.doi.org/10.1016/S0008-6215(97)00270-X). PMID:9468631.
- Lahaye, M., Inizan, F., & Vigoureux, J. (1998). NMR analysis of the chemical structure of ulvan and of ulvan-boron complex

- formation. *Carbohydrate Polymers*, 36(2-3), 239-249. [http://dx.doi.org/10.1016/S0144-8617\(98\)00026-5](http://dx.doi.org/10.1016/S0144-8617(98)00026-5).
- Li, C., Ma, H., Venkateswaran, S., & Hsiao, B. S. (2020). Highly efficient and sustainable carboxylated cellulose filters for removal of cationic dyes/heavy metals ions. *Chemical Engineering Journal*, 389, 1-13. <http://dx.doi.org/10.1016/j.cej.2019.123458>.
- Li, Y., Wang, X., Jiang, Y., Wang, J., Hwang, H., Yang, X., & Wang, P. (2019). Structure characterization of low molecular weight sulfate *Ulva* polysaccharide and the effect of its derivative on iron deficiency anemia. *International Journal of Biological Macromolecules*, 126, 747-754. <http://dx.doi.org/10.1016/j.ijbiomac.2018.12.214>. PMID:30584945.
- Lowry, O. H., Rosebrough, N. J., Farr, L., & Randall, R. J. (1951). Protein measurement with the Folin phenol reagent. *The Journal of Biological Chemistry*, 193(1), 265-275. [http://dx.doi.org/10.1016/S0021-9258\(19\)52451-6](http://dx.doi.org/10.1016/S0021-9258(19)52451-6). PMID:14907713.
- Lubambo, A. F., Ono, L., Drago, V., Mattoso, N., Varalda, J., Sierakowski, M. R., Sakakibara, C. N., Freitas, R. A., & Saul, C. K. (2015). Tuning Fe₃O₄ nanoparticle dispersion through pH in PVA/guar gum/electrospun membranes. *Carbohydrate Polymers*, 134, 775-783. <http://dx.doi.org/10.1016/j.carbpol.2015.08.013>. PMID:26428185.
- Ma, X., Liu, X., Anderson, D. P., & Chang, P. R. (2015). Modification of porous starch for the adsorption of heavy metal ions from aqueous solution. *Food Chemistry*, 181, 133-139. <http://dx.doi.org/10.1016/j.foodchem.2015.02.089>. PMID:25794731.
- Madany, M. A., Abdel-Kareem, M. S., Al-Oufy, A. K., Haroun, M., & Sheweita, S. A. (2021). The biopolymer ulvan from *Ulva fasciata*: Extraction towards nanofibers fabrication. *International Journal of Biological Macromolecules*, 177, 401-412. <http://dx.doi.org/10.1016/j.ijbiomac.2021.02.047>. PMID:33577821.
- Mahinroosta, M., Jomeh Farsangi, Z., Allahverdi, A., & Shakoobi, Z. (2018). Hydrogels as intelligent materials: A brief review of synthesis, properties and applications. *Materials Today. Chemistry*, 8, 42-55. <http://dx.doi.org/10.1016/j.mtchem.2018.02.004>.
- Mata, G. C., Morais, M. S., Oliveira, W. P., & Aguiar, M. L. (2022). Composition effects on the morphology of PVA/Chitosan electrospun nanofibers. *Polymers*, 14(22), 1-19. <http://dx.doi.org/10.3390/polym14224856>. PMID:36432987.
- Mejía Agüero, L. E., Saul, C. K., De Freitas, R. A., Rabello Duarte, M. E., & Nosedá, M. D. (2022). Electrospinning of marine polysaccharides: Processing and chemical aspects, challenges, and future prospects. *Nanotechnology Reviews*, 11(1), 3250-3280. <http://dx.doi.org/10.1515/ntrev-2022-0491>.
- Mirtič, J., Balažič, H., Zupančič, Š., & Kristl, J. (2019). Effect of solution composition variables on electrospun alginate nanofibers: Response surface analysis. *Polymers*, 11(4), 1-20. <http://dx.doi.org/10.3390/polym11040692>. PMID:30995752.
- Morelli, A., & Chiellini, F. (2010). Ulvan as a new type of biomaterial from renewable resources: Functionalization and hydrogel preparation. *Macromolecular Chemistry and Physics*, 211(7), 821-832. <http://dx.doi.org/10.1002/macp.200900562>.
- Panzavolta, S., Giofrè, M., Focarete, M., Gualandì, C., Foroni, L., & Bigi, A. (2011). Electrospun gelatin nanofibers: Optimization of genipin cross-linking to preserve fiber morphology after exposure to water. *Acta Biomaterialia*, 7(4), 1702-1709. <http://dx.doi.org/10.1016/j.actbio.2010.11.021>. PMID:21095244.
- Patil, S. V. (2008). Crosslinking of polysaccharides: Methods and applications. *Pharmaceutical Reviews*, 6(2), 1-8.
- Pelipenko, J., Kocbek, P., Govedarica, B., Rošič, R., Baumgartner, S., & Kristl, J. (2013). The topography of electrospun nanofibers and its impact on the growth and mobility of keratinocytes. *European Journal of Pharmaceutics and Biopharmaceutics*, 84(2), 401-411. <http://dx.doi.org/10.1016/j.ejpb.2012.09.009>. PMID:23085581.
- Persano, L., Camposeo, A., Tekmen, C., & Pisignano, D. (2013). Industrial upscaling of electrospinning and applications of polymer nanofibers: A review. *Macromolecular Materials and Engineering*, 298(5), 504-520. <http://dx.doi.org/10.1002/mame.201200290>.
- Petit, J.-M., & Zhu, X. X. (1996). ¹H and ¹³C NMR study on local dynamics of poly(vinyl alcohol) in aqueous solutions. *Macromolecules*, 29(6), 2075-2081. <http://dx.doi.org/10.1021/ma951502d>.
- Phan, D. N., Khan, M. Q., Nguyen, N. T., Phan, T. T., Ullah, A., Khatri, M., Kien, N. N., & Kim, I. S. (2021). A review on the fabrication of several carbohydrate polymers into nanofibrous structures using electrospinning for removal of metal ions and dyes. *Carbohydrate Polymers*, 252, 117175. <http://dx.doi.org/10.1016/j.carbpol.2020.117175>. PMID:33183622.
- Qi, X., Tong, X., Pan, W., Zeng, Q., You, S., & Shen, J. (2021). Recent advances in polysaccharide-based adsorbents for wastewater treatment. *Journal of Cleaner Production*, 315, 1-27. <http://dx.doi.org/10.1016/j.jclepro.2021.128221>.
- Ramakrishna, S., Fujihara, K., Teo, W. E., Yong, T., Ma, Z., & Ramaseshan, R. (2006). Electrospun nanofibers: Solving global issues. *Materials Today*, 9(3), 40-50. [http://dx.doi.org/10.1016/S1369-7021\(06\)71389-X](http://dx.doi.org/10.1016/S1369-7021(06)71389-X).
- Raveendran, S., Yoshida, Y., Maekawa, T., & Kumar, D. S. (2013). Pharmaceutically versatile sulfated polysaccharide based bionano platforms. *Nanomedicine; Nanotechnology, Biology, and Medicine*, 9(5), 605-626. <http://dx.doi.org/10.1016/j.nano.2012.12.006>. PMID:23347895.
- Riyajan, S. A., Chaiponban, S., & Tanbumrung, K. (2009). Investigation of the preparation and physical properties of a novel semi-interpenetrating polymer network based on epoxidised NR and PVA using maleic acid as the crosslinking agent. *Chemical Engineering Journal*, 153(1-3), 199-205. <http://dx.doi.org/10.1016/j.cej.2009.05.043>.
- Robic, A., Bertrand, D., Sassi, J. F., Lerat, Y., & Lahaye, M. (2009). Determination of the chemical composition of ulvan, a cell wall polysaccharide from *Ulva* spp. (Ulvales, Chlorophyta) by FT-IR and chemometrics. *Journal of Applied Phycology*, 21(4), 451-456. <http://dx.doi.org/10.1007/s10811-008-9390-9>.
- Robic, A., Sassi, J. F., Dion, P., Lerat, Y., & Lahaye, M. (2009). Seasonal variability of physicochemical and rheological properties of ulvan in two *Ulva* species (Chlorophyta) from the Brittany coast. *Journal of Phycology*, 45(4), 962-973. <https://doi.org/10.1111/j.1529-8817.2009.00699.x>
- Rwei, S. P., & Huang, C. C. (2012). Electrospinning PVA solution-rheology and morphology analyses. *Fibers and Polymers*, 13(1), 44-50. <http://dx.doi.org/10.1007/s12221-012-0044-9>.
- Rynkowska, E., Fatyeyeva, K., Marais, S., Kujawa, J., & Kujawski, W. (2019). Chemically and thermally crosslinked PVA-based membranes: Effect on swelling and transport behavior. *Polymers*, 11(11), 1-18. <http://dx.doi.org/10.3390/polym11111799>. PMID:31684000.
- Santos, C., Silva, C. J., Büttel, Z., Guimarães, R., Pereira, S. B., Tamagnini, P., & Zille, A. (2014). Preparation and characterization of polysaccharides/PVA blend nanofibrous membranes by electrospinning method. *Carbohydrate Polymers*, 99, 584-592. <http://dx.doi.org/10.1016/j.carbpol.2013.09.008>. PMID:24274547.
- Saravanakumar, G., Jo, D., & Park, H. (2012). Polysaccharide-based nanoparticles: A versatile platform for drug delivery and biomedical imaging. *Current Medicinal Chemistry*, 19(19), 3212-3229. <http://dx.doi.org/10.2174/092986712800784658>. PMID:22612705.
- Sari-Chmayssem, N., Taha, S., Mawlawi, H., Guégan, J. P., Jeftić, J., & Benvegnu, T. (2019). Extracted ulvans from green algae *Ulva linza* of Lebanese origin and amphiphilic derivatives: Evaluation of their physico-chemical and rheological properties. *Journal of Applied Phycology*, 31(3), 1931-1946. <http://dx.doi.org/10.1007/s10811-018-1668-y>.
- Schiffman, J. D., & Schauer, C. L. (2008). A review: Electrospinning of biopolymer nanofibers and their applications. *Polymer Reviews (Philadelphia, Pa.)*, 48(2), 317-352. <http://dx.doi.org/10.1080/15583720802022182>.
- Shaohua, H., Fumitaka, H., & Odani, H. (1990). ¹H NMR study of the solvation and gelation in a poly(vinyl alcohol)/DMSO-d₆/H₂O

- system. *Bulletin of the Institute for Chemical Research*, 67(5-6), 239-248. <http://hdl.handle.net/2433/77317>
- Shen, W., & Hsieh, Y. (2014). Biocompatible sodium alginate fibers by aqueous processing and physical crosslinking. *Carbohydrate Polymers*, 102, 893-900. <http://dx.doi.org/10.1016/j.carbpol.2013.10.066>. PMID:24507361.
- Taylor, R. L., & Conrad, H. E. (1972). Stoichiometric depolymerization of polyuronides and glycosaminoglycuronans to monosaccharides following reduction of their carbodiimide-activated carboxyl groups. *Biochemistry*, 11(8), 1383-1388. <http://dx.doi.org/10.1021/bi00758a009>. PMID:4259914.
- Terezaki, A., Kikionis, S., Ioannou, E., Sfiniadakis, I., Tziveleka, L. A., Vitsos, A., Roussis, V., & Rallis, M. (2022). Ulvan/gelatin-based nanofibrous patches as a promising treatment for burn wounds. *Journal of Drug Delivery Science and Technology*, 74, 103535. <http://dx.doi.org/10.1016/j.jddst.2022.103535>.
- Thu, T., Thanh, T., Minh, T., Quach, T., Nguyen, T. N., Luong, D. V., Bui, M. L., & Van Tran, T. T. (2016). Structure and cytotoxic activity of Ulvan extracted from green seaweed *Ulva lactuca*. *International Journal of Biological Macromolecules*, 93(Pt A), 695-702. PMID:27637450.
- Toskas, G., Hund, R. D., Laourine, E., Cherif, C., Smyrniotopoulos, V., & Roussis, V. (2011). Nanofibers based on polysaccharides from the green seaweed *Ulva rigida*. *Carbohydrate Polymers*, 84(3), 1093-1102. <http://dx.doi.org/10.1016/j.carbpol.2010.12.075>.
- Tziveleka, L. A., Ioannou, E., & Roussis, V. (2019). Ulvan, a bioactive marine sulphated polysaccharide as a key constituent of hybrid biomaterials: A review. *Carbohydrate Polymers*, 218, 355-370. <http://dx.doi.org/10.1016/j.carbpol.2019.04.074>. PMID:31221340.
- Tziveleka, L. A., Pippa, N., Georgantea, P., Ioannou, E., Demetzos, C., & Roussis, V. (2018). Marine sulfated polysaccharides as versatile polyelectrolytes for the development of drug delivery nanoplateforms: Complexation of ulvan with lysozyme. *International Journal of Biological Macromolecules*, 118(Pt A), 69-75. <http://dx.doi.org/10.1016/j.ijbiomac.2018.06.050>. PMID:29906535.
- van der Velden, G., & Beulen, J. (1982). 300-MHz ¹H NMR and 25-MHz ¹³C NMR investigations of sequence distributions in vinyl alcohol-vinyl acetate copolymers. *Macromolecules*, 15(4), 1071-1075. <http://dx.doi.org/10.1021/ma00232a022>.
- Vass, P., Szabó, E., Domokos, A., Hirsch, E., Galata, D., Farkas, B., Démuth, B., Andersen, S. K., Vigh, T., Verreck, G., Marosi, G., & Nagy, Z. K. (2020). Scale-up of electrospinning technology: Applications in the pharmaceutical industry. *Nanomedicine and Nanobiotechnology*, 12(4), e1611. PMID:31863572.
- Vigani, B., Rossi, S., Milanese, G., Bonferoni, M. C., Sandri, G., Bruni, G., & Ferrari, F. (2018). Electrospun alginate fibers: Mixing of two different poly(ethylene oxide) grades to improve fiber functional properties. *Nanomaterials (Basel, Switzerland)*, 8(12), 1-17. <http://dx.doi.org/10.3390/nano8120971>. PMID:30477265.
- Wani, S., Sofi, H. S., Majeed, S., & Sheikh, F. A. (2017). Recent trends in chitosan nanofibers: from tissue-engineering to environmental importance: A review. *Material Science Research India*, 14(2), 89-99. <http://dx.doi.org/10.13005/msri/140202>.
- Webster, E. A., Murphy, A. J., Chudek, J. A., & Gadd, G. M. (1997). Metabolism-independent binding of toxic metals by *Ulva lactuca*: Cadmium binds to oxygen-containing groups, as determined by NMR. *Biometals*, 10(2), 105-117. <http://dx.doi.org/10.1023/A:1018379106700>.
- Williams, G., Raimi-Abraham, B., & Luo, C. (2018). Electrospinning fundamentals. In G. R. Williams, C. J. Luo & B. R. Raimi-Abraham (Eds.), *Nanofibers in drug delivery* (pp. 24-59). UCL Press and JSTOR. <http://dx.doi.org/10.2307/j.ctv550dd1.6>
- Xue, J., Wu, T., Dai, Y., & Xia, Y. (2019). Electrospinning and electrospun nanofibers: Methods, materials, and applications. *Chemical Reviews*, 119(8), 5298-5415. <http://dx.doi.org/10.1021/acs.chemrev.8b00593>. PMID:30916938.
- Zhang, Y., Zhu, P. C., & Edgren, D. (2010). Crosslinking reaction of poly(vinyl alcohol) with glyoxal. *Journal of Polymer Research*, 17(5), 725-730. <http://dx.doi.org/10.1007/s10965-009-9362-z>.

Supplementary Material

Supplementary material accompanies this paper.

Table S1. Recovery, M_w , chemical analyses, and specific rotation of U and carboxy-reduced U (UR*) from *U. fasciata*.

Table S2. Monosaccharide composition of U and carboxy-reduced U (UR*) from *U. fasciata*.

Table S3. ^1H NMR chemical shift assignments of U.

Table S4. ^1H chemical shifts assignments for PVA dissolved in DMSO- d_6 and D $_2\text{O}$.

Table S5. ^1H NMR chemical shift assignments for PVA5U2 dissolved in D $_2\text{O}$.

Figure S1. Fibers produced by spinning U/PVA blends in two different mass ratios: (a) 5:2 and (b) 3:5.

Figure S2. G' and G'' as a function of shear stress (constant frequency 1Hz) at 20 °C for: (a) mixture U/PVA (PVA5U2), (b) U 2 wt % solution, (c) PVA 5 wt % solution.

Figure S3. Edge effect and rheological behavior.

Figure S4. ^1H NMR spectrum of U (2wt% solution in D $_2\text{O}$. *Acetone as internal reference at 70°C).

Figure S5. ^1H NMR spectrum of PVA (5wt% solution in D $_2\text{O}$. *Acetone as internal reference at 70°C).

Figure S6. (a) ATR-FTIR spectrum of U, (b)ATR-FTIR spectrum of PVA5U2 mat.

Figure S7. Comparison between ATR-FTIR spectra of PVA5U2 mat and U extract.

Figure S8. ATR-FTIR spectrum of PVA powder.

Figure S9. Comparison between ATR-FTIR spectra of PVA5U2 mat and PVA powder.

Figure S10. PVA5U2 crosslinked nanofiber mat after impregnation with a ferric chloride solution PVA5U2 mat swelling and dissolution rate measurements.

This material is available as part of the online article from <https://doi.org/10.4322/biori.00162023>